Proc. Natl. Acad. Sci. USA
Vol. 89, pp. 10262–10266, November 1992
Physiology

Mouse cortical collecting duct cells show nonselective cation channel activity and express a gene related to the cGMP-gated rod photoreceptor channel

(kidney/patch-clamp/polymerase chain reaction)

IQBAL AHMAD*, CHRISTOPH KORBMACHER†‡, ALAN S. SEGAL†, PAMELA CHEUNG*, EMILE L. BOULPAEP†§, AND COLIN J. BARNSTABLE*

Departments of *Ophthalmology and Visual Science and †Cellular and Molecular Physiology, Yale University School of Medicine, 333 Cedar Street, New Haven, CT 06510

Communicated by Gerhard Giebisch, June 16, 1992

ABSTRACT **Apical nonselective cation channels with an average single-channel conductance of 34 ± 2.3 pS were found in M-1 mouse cortical collecting duct cells. Channel activity is increased by depolarization and abolished by cytoplasmic calcium removal. Cytoplasmic application of 0.1 mM cGMP decreases channel open probability by 27%. cDNAs corresponding to ≈40% of the coding region of the photoreceptor channel were isolated by the polymerase chain reaction from M-1 cells and a rat kidney cDNA library. The rat kidney-derived sequence differs by a single base, and the M-1-cell-derived sequence differs by only two bases, from the photoreceptor sequence. A second clone from M-1 cells differs by 20 out of 426 bases from the photoreceptor sequence. In all three clones, the deduced amino acid sequence is identical to that of the rat photoreceptor channel. Northern blot analysis of poly(A)$^+$ RNA from M-1 cells reveals the presence of a 3.2-kilobase band hybridizing with a retinal cGMP-gated cation channel probe. The results suggest the expression in M-1 cells of more than one gene coding for nonselective cation channels or channel subunits, one of which is identical to the cGMP-gated cation channel gene of rod photoreceptors.**

Nonselective cation channels in a large variety of excitable and nonexcitable tissues show a high selectivity for cations over anions but discriminate poorly between sodium and potassium (1, 2). The cGMP-gated vertebrate photoreceptor channel, which mediates the electrical response to light, is a nonselective cation channel (3). The cloned cDNA for this channel, expressed in *Xenopus* oocytes, gives rise to a cGMP-gated cation channel with properties of the photoreceptor channel (4). Both electrophysiological and biochemical studies suggest that this channel is also expressed in retinal bipolar and ganglion cells (5, 6).

A closely related protein has been isolated from olfactory epithelium (7). Further evidence for a gene family has been obtained from Northern blot analysis by using a probe from the rod photoreceptor channel (8). A transcript of the same size as the retinal RNA was found in rat heart and kidney but not in muscle, thymus, spleen, or liver.

The presence of renal mRNA that hybridized to a retinal cGMP-gated channel probe is of interest, since nonselective cation channels have been detected electrophysiologically in the proximal tubule (9, 10), in cortical thick ascending limb cells (11), and in collecting duct cells (12–14). Furthermore, cGMP seems to play a role in the regulation of the nonselective cation channel in the inner medullary collecting duct (15, 16).

The M-1 cell line used in the present study maintains epithelial transport properties characteristic of the collecting duct *in vivo* (17). We now report the presence of nonselective cation channels in M-1 cells. Furthermore, reverse transcription–PCR amplification was used to detect and clone sequences related to the cGMP-gated rod photoreceptor channel from M-1 cells and from rat kidney.¶

MATERIALS AND METHODS

Cell Culture. The M-1 cell line was originally derived from a microdissected cortical collecting duct of a mouse transgenic for the early region of simian virus 40 [strain Tg (SV40) Bri/7] (17) and was a gift of G. Fejes-Toth. Cells used in the present study were from passages 7–12 and were maintained in PC1 medium (Ventrex Laboratories, Portland, ME) (17). For patch-clamp experiments, cells grown on glass coverslips were used 1–17 days after seeding. For RNA preparation, subconfluent or confluent M-1 cells grown on plastic culture dishes were harvested 3–20 days after seeding.

Patch-Clamp Experiments. The inside-out configuration of the patch-clamp technique was used (18), and single-channel currents were amplified with a List EPC-7 patch-clamp amplifier (List Electronics, Darmstadt, F.R.G.) and recorded as described (19). Currents were filtered at 1 kHz for analysis. Software for data acquisition and analysis was written in our laboratory. Bath solutions (at pH 7.5) were NaCl/Ringer's (140 mM NaCl, 5 mM KCl, 1 mM $CaCl_2$, 1 mM $MgCl_2$, 5 mM glucose, and 10 mM Hepes buffered with NaOH), KCl/Ringer's (140 mM KCl, 5 mM NaCl, 1 mM $CaCl_2$, 1 mM $MgCl_2$, 5 mM glucose, and 10 mM Hepes buffered with KOH), and sucrose/Ringer's (10 mM NaCl, 5 mM KCl, 1 mM $CaCl_2$, 1 mM $MgCl_2$, 260 mM sucrose, 5 mM glucose, and 10 mM Hepes buffered with NaOH). A free calcium concentration of <1 nM was obtained by including 1 mM EGTA instead of 1 mM $CaCl_2$. Freshly prepared cGMP (Sigma) was added to the bath from a 10 mM aqueous stock solution. Pipette solutions were either KCl/Ringer's, NaCl/Ringer's, or a Na_2SO_4/K_2SO_4/Ringer's, which contained 12.5 mM NaCl, 30 mM Na_2SO_4, 12.5 mM KCl, 30 mM K_2SO_4, 60 mM sucrose, and 10 mM Hepes adjusted to pH 7.5 with NaOH/KOH.

cDNA Isolation. RNA for cDNA synthesis (total RNA) and for Northern analysis [poly(A)$^+$ RNA] was isolated as described (8, 20). Primers for PCR amplification were chosen to correspond to the sequence of conserved regions of the rat rod photoreceptor cGMP-gated ion channel (21). For cloning

The publication costs of this article were defrayed in part by page charge payment. This article must therefore be hereby marked "*advertisement*" in accordance with 18 U.S.C. §1734 solely to indicate this fact.

Abbreviations: P_o, open-state probability; N, number of channels in a membrane patch; I–V, current–voltage.

‡Present address: Zentrum der Physiologie, Johann Wolfgang Goethe Universität, Theodor Stern Kai, 7, D-6000, Frankfurt 70, Federal Republic of Germany.
§To whom reprint requests should be addressed.

¶The sequences reported in this paper have been deposited in the GenBank data base (accession nos. L02635 and L02636).

purposes, the forward and reverse primers in each set began with *Eco*RI and *Hin*dIII sites, respectively. All primers were synthesized on an automated DNA synthesizer (Applied Biosystems model 391) and were used after purification over Sephadex G-50. First-strand cDNA synthesis and PCR amplification were as described (20). PCR amplification was also carried out on aliquots of a rat kidney cDNA library (Clontech; no. RL1031). The cDNAs amplified by PCR were concentrated, digested overnight with *Eco*RI and *Hin*dIII, ligated into complementarily digested Bluescript (Stratagene) vector, and transformed into bacterial host by using standard techniques (22). Putative positive clones were analyzed by restriction digest analyses followed by sequencing on both strands of DNA (23). Electrophoretic resolution of RNA and hybridization for Northern analyses were as described (20).

RESULTS

Apical Nonselective Cation Channels in M-1 Cells. Fig. 1*A* shows the outward current trace for an inside-out patch containing at least six channels. Discrete current levels are seen in the amplitude histogram obtained from 18 s of continuous current record (Fig. 1*B*). Similar amplitude histograms were used to calculate single-channel unitary currents at different holding potentials to yield a current–voltage (*I–V*) relationship. In NaCl/Ringer's bath solution, the *I–V* relationship can be fitted by a linear regression, which reveals a reversal potential of −0.3 mV and single-channel conductance of 46 pS (Fig. 1*C*). This reversal potential suggests a nonselective channel, since under these conditions E_K is +72 mV, E_{Na} is −18 mV, and E_{Cl} is +48 mV. When the bath was changed to KCl/Ringer's solution the *I–V* plot was nearly identical, with a reversal potential of −1.8 mV and a conductance of 50 pS (Fig. 1*C*), indicating a sodium-to-potassium permeability ratio of ≈1. When the bath was either NaCl/Ringer's solution or KCl/Ringer's solution, single-channel conductances averaged 34 ± 2.3 pS (n = 27). Fig. 1*D* shows a bath salt dilution where sucrose/Ringer's solution replaced KCl/Ringer's solution to demonstrate the cation versus anion selectivity of the channel. The *I–V* data were

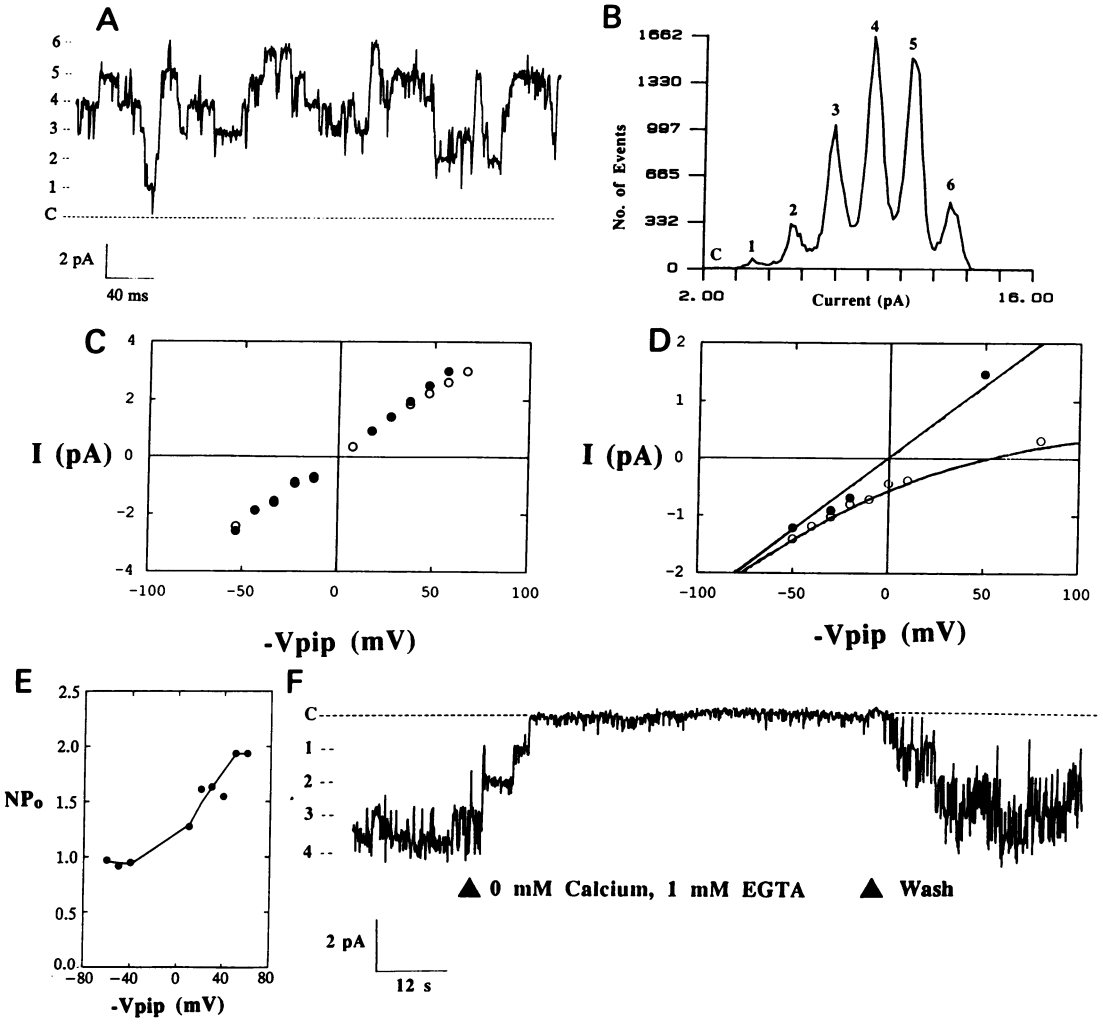

FIG. 1. Inside-out apical patches from M-1 cell. The trans-patch potential difference is the negative holding potential ($-V_{pip}$), or cytoplasmic potential referred to pipette potential. The pipette solution was Na_2SO_4/K_2SO_4/Ringer's unless indicated otherwise. (*A*) Current record of nonselective cation channels at $-V_{pip}$ = 27 mV. Upward deflections indicate outward currents. The bath solution was NaCl/Ringer's. (*B*) Amplitude histogram of 18,329 ms of current record (45,823 samples) in 140 bins of 0.1-pA width. Peak separation indicates single-channel current of 1.66 pA at $-V_{pip}$ = 27 mV. (*C*) Single-channel *I–V* plot. ○, NaCl/Ringer's solution in bath; ●, KCl/Ringer's solution in bath. (*D*) *I–V* plots of a single-channel record in an inside-out membrane patch. The pipette solution was NaCl/Ringer's. ●, KCl/Ringer's solution in bath. The data were fitted by using the Goldman–Hodgkin–Katz equation for symmetrical 150 mM cations and 25-pS conductance. ○, Sucrose/Ringer's solution in bath. The data were fitted by using the Goldman–Hodgkin–Katz equation for a cation ratio of 20 mM/150 mM (E_{rev} = 54 mV) and a reference conductance of 25 pS. (*E*) Voltage dependence of the open probability (NP_o). The pipette solution was KCl/Ringer's; the bath solution was NaCl/Ringer's. (*F*) Effect of calcium removal from bath on nonselective cation channel activity in an inside-out patch at $-V_{pip}$ = −40 mV. Downward deflections indicate inward current. The pipette solution was NaCl/Ringer's; the bath solution was KCl/Ringer's.

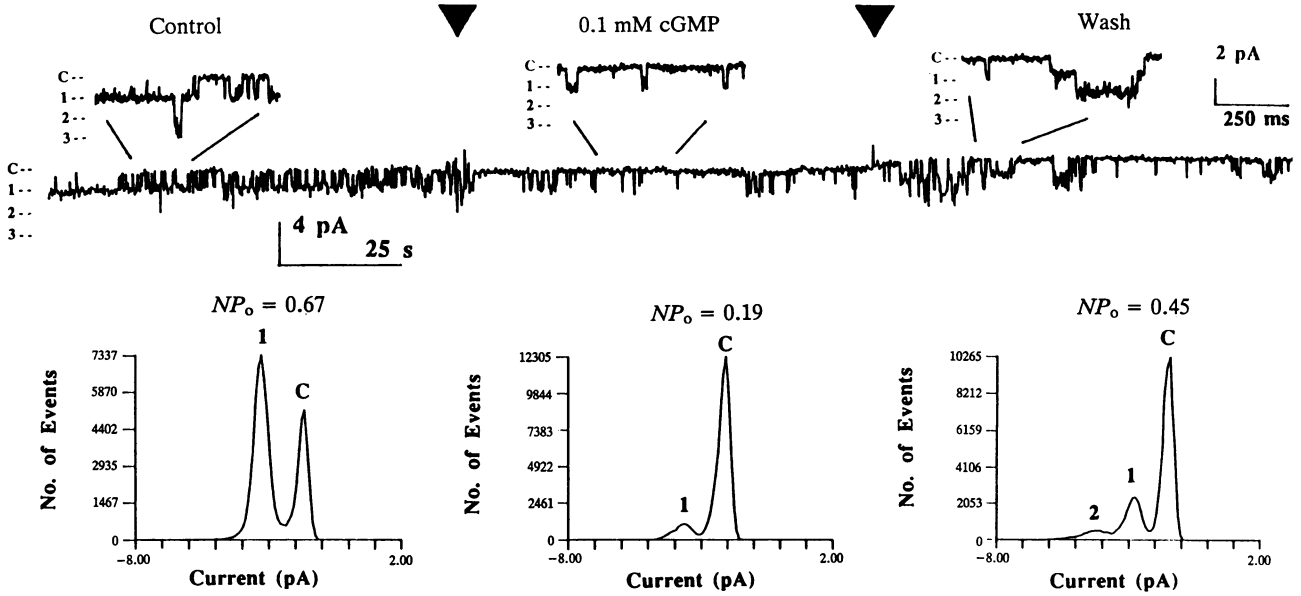

FIG. 2. Effect of 0.1 mM cGMP on a continuous record of nonselective cation channel activity in an inside-out patch at $-V_{pip} = -50$ mV. Downward deflections indicate inward current. cGMP (0.1 mM) was present between the arrowheads. Insets show current records on a faster time base. Horizontal bars indicate three 80-s intervals of record from which amplitude histograms were generated. NP_o values are given above each histogram.

fitted using the Goldman–Hodgkin–Katz constant-field equation and the asymptotic conductance of 25 pS. By assuming a reversal potential of +40 to +50 mV in sucrose/Ringer's solution, the calculated cation-to-chloride permeability ratio ranges from 11 to 48.

The product NP_o is the number of channels in the patch (N) times the open-state probability (P_o) of each channel. NP_o for these nonselective channels was higher at depolarizing transpatch potentials than at hyperpolarizing potentials (Fig. 1*E*). Fig. 1*F* shows that calcium removal reversibly abolished channel activity ($n = 5$).

Fig. 2 illustrates that application of 0.1 mM cGMP resulted in a 72% reduction of NP_o with a subsequent recovery after cGMP washout to 67% of the original value. Results of 14 similar experiments are given in Table 1. NP_o values for the different periods of an experiment (control, cGMP, and washout) were calculated with current amplitude histograms generated from continuous current records. The analyzed time intervals averaged 62.2 ± 3.5 s. NP_o decreased in 10 out of 14 experiments in the presence of 0.1 mM cGMP, as compared to the prior control period. After washout of cGMP, NP_o showed partial recovery in five cases. In 3 of the 10 experiments, channel activity ceased completely either during the cGMP application or after washout and did not recover thereafter. In 4 out of 14 experiments, cGMP appeared to increase channel activity, although in 2 experiments NP_o continued to increase even after cGMP washout. When the data were normalized by dividing NP_o by an estimate of the lower limit of the number of channels (N), P_o averaged 0.40 ± 0.09 in control versus 0.29 ± 0.07 in the presence of 0.1 mM cGMP ($n = 14$, mean ± SEM). The paired differences of the P_o values obtained in the presence of 0.1 mM cGMP and the prior control period averaged −0.11 ± 0.05 ($P = 0.05$ in paired t test). Thus, 0.1 mM cGMP decreased channel activity by 27%.

Table 1. Effect of 0.1 mM cGMP on the NP_o of the nonselective cation channel in M-1 mouse cortical collecting duct cells

No.	NP_o Control	NP_o cGMP	NP_o Washout	% change*	g, pS	N
1	7.06	3.85	4.77	−45.5	24	10
2	3.30	2.85	3.82	−13.6	46	6
3	2.89	0.92	0.95	−68.2	19	3
4	1.64	1.38	1.61	−15.9	26	2
5	0.67	0.19	0.45	−71.2	34	3
6	0.96	0.95	—	−1.0	17	2
7	0.13	0.07	—	−46.2	20	3
8	3.38	2.69	0	−20.4	44	4
9	0.34	0.22/0	0	−35.3	40	4
10	0.14	0	0	−100	37	2
11	1.63	1.72	1.93	+5.5	16	3
12	0.39	0.58	1.19	+48.7	25	9
13	0.76	0.89	—	+17.1	40	5
14	0.15	0.24	—	+60.0	40	2

g, channel conductance.
*[(cGMP NP_o − control NP_o)/control NP_o] × 100%.

Detection of cGMP-Gated Cation Channel Transcripts in M-1 Cells. Single-stranded cDNA was prepared from total RNA of M-1 cells. Aliquots of this cDNA, and of a rat kidney cDNA library, were then used in PCR reactions using oligonucleotide primers complementary to the rod retinal cGMP-gated cation channel (Fig. 3). Although no band could be seen in either case by ethidium bromide staining, strong bands consistent with the predicted size of 458 base pairs (bp) were observed when aliquots of the PCR reactions were further amplified with primer set B. A Southern analysis showed that

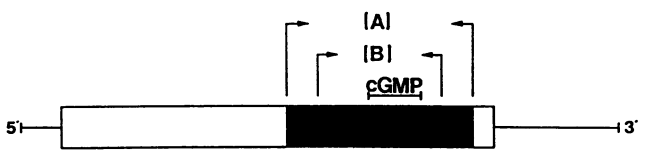

FIG. 3. Schematic diagram of rat rod photoreceptor cDNA showing the positions of the forward and reverse primers used. Primer set A [5'-GCCACCATTGTCGGTAACATAGGCTCCATG-3' (forward) and 5'-TCATACTCAGCCAAGATTCGGGCA-3' (reverse)] was chosen to amplify a 788-bp sequence comprising about 40% of the coding sequence. Primer set B [5'-ATTAAATGGTT-TGAC-3' (forward) and 5'-CTCTGTAAGAGCTTCCAT-3' (reverse)] was chosen to amplify a 458-bp sequence within the sequence amplified by primer set A. The position of the putative cGMP binding region is also shown.

```
Rat retina  ATTTCCAATATGAATGCAGCCCGGGCAGAATTTCAATCAAGAGTTGATGCTATCAAACAGTACATGAATTTTCGAAATGTGAGCAAAGACATGGAAAAGAGAGTTATTAAATGGTTTGACT
Rat olf     --C-----C--------CA-A--A-----G--C--GG-C-AGA--------G-------C------C-G--C-----G--C---------------GCC-AG--C--C-------------
Rat kidney  ----------------------------------------------------------------------------------------------------------------------------
M1 clone 1  ----------------------------------------------------------------------------------------------------------------------------

Rat retina  ACCTGTGGACCAACAAAAAGACAGTCGATGAGAGAGAAGTTCTGAGATACCTCCCTGACAAACTCAGGGCAGAGATTGCCATCAATGTTCACCTAGACACGTTAAAAAAGGTTCGTATCTT
Rat olf     --T----------T--G--------A-----AC-------C--C-AGA----G--A-CA--G--------T-----A-----T---------T-GTC---TC-G--G--A--G--C--A--
Rat kidney  ----------T-----------------------------------------------------------------------------------------------------------
M1 clone 1  ----------T-----------------------------------------------------------------------------------G-----------------------
M1 clone 2  --------------------A-----G--------------C----------------------A--------A----------C-----T-----------------------C-----

Rat retina  TGCTGACTGTGAGGCTGGTCTGTTGGTGGAGTTGGTGTTGAAATTACAACCCCAGGTGTACAGTCCTGGAGATTACATATGCAAGAAAGGGGACATTGGGCGGGAGATGTACATCATCAAG
Rat olf     CCAGGAT-----A-----C--AC-------AC----AC----GC-T-GT--T-----C-TT--------------T--T---CGT--G----------CAA---A--------------
Rat kidney  ----------------------------------------------------------------------------------------------------------------------------
M1 clone 1  ----------------------------------------------------------------------------------------------------------------------------
M1 clone 2  -----------A----------------------------C---------------T-----C----------------------------C-------------------------

Rat retina  GAAGGCAAACTTGCTGTGGTGGCAGACGACGGAATCACACAGTTTGTGGTGTTGAGTGACGGCAGCTACTTTGGCGAGATCAGCATTCTTAACATCAAAGGCAGCAAGGCTGGCAACCGAA
Rat olf     --G-----GT-G--A-----A--T--T--T--CG-G--T----A--CCT--C-CTCA-CT--G----G------T-----T--T--C--------T--G--T-----AATG-----T---C
Rat kidney  ----------------------------------------------------------------------------------------------------------------------------
M1 clone 1  ----------------------------------------------------------------------------------------------------------------------------
M1 clone 2  -------------------------T--------T----------------------------T--------T----------------T-------------------------

Rat retina  GAACAGCCAATATTAAGAGCATTGGCTACTCGGACCTGTTCTGCCTCTCAAAGGATGACCTCATGGAAGCTCTTACAGAGTACCCAGATGCCAAAACTATGTTGGAGGAGAAAGGGAGGCA
Rat olf     -T--T--T-----CCGT---C-G--------A--T--C------T-G--C-----C--T--T---------G-A--T-----T--T--------G-AGG-CC-------ACGG--T---G-
Rat kidney  ----------------------------------------------------------------------------------------------------------------------------
M1 clone 1  ----------------------------------------------------------------------------------------------------------------------------
M1 clone 2  ----------C----------C-----------------------------------------

Rat retina  GATCTTAATGAAAGACGGTCTACTGGATATAAACATTGCGAATTTGGGCAGTGACCCTAAAGCCTGGGAAGAGAAGGTCACTCGAATGGAGGGGTCAGTGGACCTCCTGCAAACACGATT
Rat olf     ----C-G-----G--A----------GAG--TGAA-T-GCAGCTA-T-TG--GGTAG-T-TTCA---GA--CT--AACAGTTGGA-ACAAACATG-ATAC-T-GTACACTCGCTTTGC
Rat kidney  ----------------------------------------------------------------------------------------------------------------------------
M1 clone 1  ----------------------------------------------------------------------------------------------------------------------------
```

FIG. 4. Sequences of cDNAs cloned from rat kidney and M-1 cells compared with the sequence of the cyclic nucleotide-gated ion channel from rat rod photoreceptor (rat retina) and rat olfactory epithelium (rat olf). Dashes show identities with the rod photoreceptor sequence. M-1 clone 2 was derived from primer set B and is thus shorter than the other sequences. The sequences of oligonucleotides used in the PCR reactions have not been included in this figure.

these bands reacted with a probe corresponding to the rat rod cGMP-gated channel.

The PCR amplification products were cloned into Bluescript vector, the inserts were completely sequenced, and the sequences were compared with those of the rat rod channels and the rat olfactory channel (Fig. 4). The sequence cloned from the rat kidney cDNA library differed by only 1 base from the rat rod sequence. Two sequences were derived from the M-1 clones. One sequence was almost identical to that of the rat kidney and differed from the rod sequence by 2 bases. The second sequence showed more variation and differed from the rat rod sequence by 20 out of 426 bases. All differences found were in redundant positions and thus gave a deduced amino acid sequence identical to that of the rod channel.

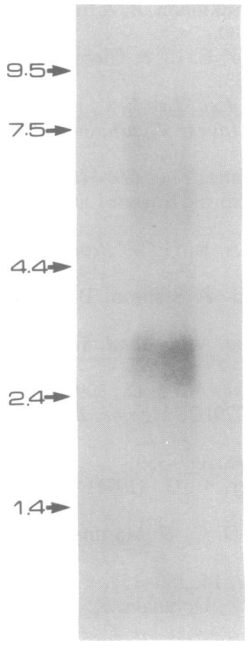

FIG. 5. Northern blot analysis of the cGMP-gated ion channel in M-1 cells. Poly(A)$^+$ RNA (30 μg) obtained from M-1 cells was electrophoresed and hybridized with ^{32}P-labeled cDNA corresponding to the cGMP-binding region of the rat rod photoreceptor cGMP channel. An RNA ladder was used to estimate molecular size (in kilobases).

The cGMP-gated cation channel in rat rods is translated from a 3.2-kilobase mRNA. Northern blot analysis of poly(A)$^+$ RNA from M-1 cells also revealed the presence of a 3.2-kilobase band hybridizing with a retinal cGMP-gated cation channel probe (Fig. 5).

DISCUSSION

Nonselective cation channels in apical membrane patches of M-1 cells do not discriminate between sodium and potassium, have a linear single-channel *I–V* relationship, and have an average single-channel conductance of 34 pS. NP_o of the channels increases with depolarization, and channel activity is abolished upon removal of calcium on the cytoplasmic side of the patch. The channel described in the present study is similar to the nonselective cation channel previously described in various collecting duct cells (12–14), including M-1 cells (24).

Small-conductance amiloride-sensitive apical channels, which are highly selective for sodium (25, 26), are probably the major route for Na^+ reabsorption in the collecting duct epithelium (27). In the inner medullary collecting duct, the nonselective cation channel has been shown to be sensitive to submicromolar concentrations of amiloride (12). cGMP can reduce NP_o of the inner medullary collecting duct channel directly as well as indirectly via a cGMP-dependent protein kinase (15, 16). The channel may also be regulated by atrial natriuretic peptide via guanylate cyclase activation. Hence, the inner medullary collecting duct channel may play a role in sodium reabsorption (15, 16). In contrast, the nonselective cation channel in cultured rabbit cortical collecting duct cells is insensitive to amiloride, which argues against a role in Na^+ reabsorption (13). Highly sodium-selective channels and nonselective cation channels may coexist in the same cell type (13, 24).

In M-1 cells, 0.1 mM cGMP decreases channel activity by 27%. However, this average decrease includes experiments in which cGMP actually led to a rise in channel opening. Thus, our findings are consistent with preliminary experi-

ments on M-1 cells in which 0.1 mM cGMP reduced channel NP_o by 54% (24). Whereas in 10 out of 14 experiments NP_o decreased after cGMP addition, in 4 experiments we observed an increase in NP_o. In 2 of these, NP_o continued to increase after cGMP washout. Nonselective channels are known to have nonstationary kinetics with spontaneous changes of their activity in clusters of openings, sometimes separated by prolonged closings of many minutes (28). Thus, spontaneous changes in channel activity, occurring simultaneously with changes induced by an experimental maneuver, complicate the interpretation of the data. Finally, cGMP has been shown to have stimulatory rather than inhibitory effects on nonselective cation channels in toad urinary bladder (29) and in excised membrane patches of A6 cells (30).

The presence or absence of factors such as membrane-bound protein kinases or certain substrates in an individual membrane patch microenvironment may also be responsible for the variability of the cGMP effect observed in the present study. In three experiments, complete channel shutdown was observed following cGMP application. This result would be consistent with the presence of a cGMP-dependent protein kinase in the patch, since exogenous cGMP-dependent protein kinase has been shown to cause channel shutdown in inner medullary collecting duct cells (15).

Over a region of 788 bp, about 40% of the coding sequence including the putative cGMP binding site, cDNAs cloned from M-1 cells and a rat kidney library differed from the rat rod sequence by 2 and 1 bp, respectively (4, 8). None of these differences affect the deduced amino acid sequence. This strong conservation over such a large portion of the coding region would not be expected for tissue-specific members of a gene family. For example, the rat rod photoreceptor and olfactory channel sequences differ by 33% over the same 788-bp region. The minor differences between rat kidney or M-1 sequence and the rat rod sequence are more likely due to polymorphic and species variation. Thus, one of the genes encoding a nonselective cation channel subunit in M-1 cells and rat kidney appears to be identical to the gene expressed in rod photoreceptors. This conclusion is supported by the finding of a sequence corresponding to 61% of the 3′ untranslated region of the rod channel expressed in both rat kidney and M-1 cells that differed by only one base (data not shown).

A second sequence obtained from M-1 cells differed from that of the rat rod channel by 20 out of 426 bases (4.7%). These differences were not scattered randomly since none of them altered the amino acid sequence. Thus, they are unlikely to be the result of a PCR or cloning artifact. It is far more likely that the sequence represents a different gene expressed in M-1 cells.

Pending expression of full-length sequences, we cannot be sure that our cDNAs encode the channels observed in the patch-clamp studies. In fact there are striking differences in physiological properties between the rod photoreceptor and kidney nonselective cation channels. cGMP increases the NP_o of the rod channel, but it decreases the NP_o of the nonselective cation channel in inner medullary collecting duct cells (15, 16) and in M-1 cells. The channels are also affected differently by divalent cations. In the photoreceptor channel, the single-channel conductance in the absence of Ca^{2+} or Mg^{2+} is 20–25 pS and decreases to ≈0.1 pS in the presence of 1 mM Ca^{2+} or Mg^{2+}. In contrast, the channel in M-1 cells is active in the presence of 1 mM Ca^{2+} and 1 mM Mg^{2+}, whereas calcium removal abolishes channel activity. Nevertheless, similarities exist between the photoreceptor and the M-1 cell channels: a similar single-channel conductance, a similar selectivity for monovalent cations with a Na^+-to-K^+ permeability ratio of ≈1, a linear single-channel *I–V* relationship, and an increase in NP_o at depolarized voltages (31).

The sequence of the rod photoreceptor channel shows some degree of homology with voltage-gated potassium channels, suggesting that it shares the proposed model of four subunits each with six transmembrane helices and a β-barrel lining the channel pore (32). If a similar structure exists for the kidney nonselective cation channel, our suggestion that multiple subunits may exist in M-1 cells implies that channels may be heteromers. Whether the channel also has a heteromeric structure in the retina remains to be determined.

This work was supported by Grants DK-13844, DK-17433, EY-05206, and NS-20483 from the National Institutes of Health, a Forschungsstipendium of the Deutsche Forschungsgemeinschaft to C.K., a Brown–Coxe fellowship from Yale University to I.A., and a Burroughs Wellcome Fund/National Kidney Foundation Research Fellowship to A.S.

1. Partridge, L. D. & Swandulla, D. (1988) *Trends Neurosci.* **11**, 69–72.
2. Cook, D. J., Poronnik, P. & Young, J. A. (1990) *J. Membr. Biol.* **114**, 37–52.
3. Yau, K.-W. & Baylor, D. A. (1989) *Annu. Rev. Neurosci.* **12**, 289–327.
4. Kaupp, U. B., Niidome, T., Tanabe, T., Terada, S., Bönigk, W., Stühmer, W., Cook, N. J., Kangawa, K., Matsuo, H., Hirose, T., Miyata, T. & Numa, S. (1989) *Nature (London)* **342**, 762–766.
5. Nawy, S. & Jahr, C. E. (1991) *Neuron* **7**, 677–683.
6. Ahmad, I., Cummins, D. & Barnstable, C. J. (1992) *Invest. Ophthalmol. Vis. Sci.*, Suppl. 33, 940.
7. Dhallan, R. S., Yau, K.-W., Schrader, K. A. & Reed, R. R. (1990) *Nature (London)* **347**, 184–187.
8. Ahmad, I., Redmond, L. J. & Barnstable, C. J. (1990) *Biochem. Biophys. Res. Commun.* **173**, 463–470.
9. Filipovic, D. & Sackin, H. (1991) *Am. J. Physiol.* **260**, F119–F129.
10. Gögelein, H. & Greger, R. (1986) *Pflügers Arch.* **407**, Suppl. 2, S142–S148.
11. Merot, J., Poncet, V., Bidet, M., Tauc, M. & Poujeol, P. (1991) *Biochim. Biophys. Acta* **1070**, 387–400.
12. Light, D. B., McCann, F. V., Keller, T. M. & Stanton, B. A. (1988) *Am. J. Physiol.* **255**, F278–F286.
13. Laskowski, F. H., Christine, C. W., Gitter, A. H., Beyenbach, K. W., Gross, P. & Frömter, E. (1990) *Renal Physiol. Biochem.* **13**, 70–81.
14. Ling, B. N., Hinton, C. F. & Eaton, D. C. (1991) *Kidney Int.* **40**, 441–452.
15. Light, D. B., Corbin, J. D. & Stanton, B. A. (1990) *Nature (London)* **344**, 336–339.
16. Light, D. B., Schwiebert, E. M., Karlson, K. H. & Stanton, B. A. (1989) *Science* **243**, 383–385.
17. Stoos, B. A., Naray-Fejes-Tóth, A., Carretero, O. A., Ito, S. & Fejes-Tóth, G. (1991) *Kidney Int.* **39**, 1168–1175.
18. Hamill, O. P., Marty, A., Neher, E., Sakmann, B. & Sigworth, F. J. (1981) *Pflügers Arch.* **391**, 85–100.
19. Hunter, M., Lopes, A. G., Boulpaep, E. L. & Giebisch, G. (1986) *Am. J. Physiol.* **251**, F725–F733.
20. Ahmad, I. & Barnstable, C. J. (1992) *Exp. Eye Res.*, in press.
21. Barnstable, C. J. & Ahmad, I. (1991) *Invest. Ophthalmol. Vis. Res.* **32**, Suppl., 847.
22. Sambrook, J., Fritsch, E. F. & Maniatis, T. (1989) *Molecular Cloning: A Laboratory Manual* (Cold Spring Harbor Lab., Cold Spring Harbor, NY), 2nd Ed.
23. Sanger, S., Nicklen, S. & Coulson, A. R. (1977) *Proc. Natl. Acad. Sci. USA* **74**, 5463–5467.
24. Kizer, N., Hu, J.-M., Fejes-Tóth, G. & Stanton, B. (1991) *FASEB J.* **5**, A689 (abstr.).
25. Palmer, L. G. & Frindt, G. (1986) *Proc. Natl. Acad. Sci. USA* **83**, 2767–2770.
26. Garty, H. & Benos, D. J. (1988) *Physiol. Rev.* **68**, 309–373.
27. O'Neil, R. G. & Boulpaep, E. L. (1979) *J. Membr. Biol.* **50**, 365–387.
28. Yellen, G. (1982) *Nature (London)* **296**, 357–359.
29. Das, S., Garepapaghi, M. & Palmer, L. G. (1991) *Am. J. Physiol.* **260**, C234–C241.
30. Ohara, A., Matsumoto, P., Eaton, D. C. & Marunaka, Y. (1991) *FASEB J.* **5**, A689 (abstr.).
31. Kaupp, U. B. (1991) *Trends Neurosci.* **14**, 150–157.
32. Guy, H. R., Durell, S. R., Warmke, J., Drysdale, R. & Ganetzky, B. (1991) *Science* **254**, 730.